10 Years of Stellar Activity for GJ 1243

James. R. A. Davenport,[1] Guadalupe Tovar Mendoza,[1,2] and Suzanne L. Hawley[1]

[1]*Astronomy Department, University of Washington, Box 951580, Seattle, WA 98195, USA*
[2]*Astrobiology Program, University of Washington, 3910 15th Ave. NE, Box 351580, Seattle, WA 98195, USA*

ABSTRACT

The flaring M4 dwarf GJ 1243 has become a benchmark for studying stellar flare and starspot activity thanks to the exceptional photometric monitoring archive from the *Kepler* mission. New light curves from the TESS mission for this star allow precise stellar activity characterization on more than a decade timescale. We have carried out the first flare and starspot analysis of GJ 1243 from over 50 days of data from TESS Sectors 14 and 15. Using 133 flare events detected in the 2-minute cadence TESS data, we compare the cumulative flare frequency distributions, and find the flare activity for GJ 1243 is unchanged between the *Kepler* and TESS epochs, revealing no sign of a stellar activity cycle over this decade. Two distinct starspot groups are found in the TESS data, with the primary spot having the same rotational period and phase as seen in *Kepler*. The phase of the secondary spot feature is consistent with the predicted location of the secondary starspot and measurement of weak differential rotation by Davenport et al. (2015), suggesting this secondary spot may be long-lived and stable in both latitude and longitude.

1. INTRODUCTION

The rapidly rotating, magnetically active, M4 star GJ 1243 is perhaps one of the best characterized flare stars over the past decade. Four years of nearly continuous 30-minute cadence observations by the *Kepler* mission (Borucki et al. 2010) found prominent starspots for GJ 1243 (*Kepler* ID 9726699) rotating with a period of 0.59 days (Savanov & Dmitrienko 2011), and with indications of very slow starspot evolution due to weak differential rotation (Davenport et al. 2015; Giles et al. 2017). *Kepler* also obtained 11 months of "short cadence" (1-minute) monitoring, which were ideal for characterizing the flare activity for this star (Hawley et al. 2014; Silverberg et al. 2016), amassing the largest catalog of homogeneously observed flares for any star besides the Sun (Davenport et al. 2014). As the brightest single flaring M dwarf in the *Kepler* field, GJ 1243 has become the benchmark flare star studied by exoplanet-searching telescopes.

The Transiting Exoplanet Survey Satellite (hereafter TESS Ricker et al. 2014), in many ways the successor to *Kepler*, has recently revisited GJ 1243 (TESS ID 273589987). Short-cadence (2-minute) light curves for GJ 1243 are available from Sectors 14 and 15, providing the most detailed light curve for this star since the end of the *Kepler* mission, and giving a 10-year baseline since the first *Kepler* data became available (30-minute cadence data from *Kepler* Quarter 0 in 2009).

Corresponding author: James. R. A. Davenport
jrad@uw.edu

The decade timescale of precision photometric monitoring using the combined *Kepler*–TESS data enables a host of new stellar activity studies. Most notably, this provides stellar activity estimations (e.g. starspot amplitudes and rotation rates, and flare activity levels) on a timescale that is comparable to the Sun's ∼11 yr activity cycle. As Scoggins et al. (2019) has recently highlighted, variations in flare rates determined with missions like *Kepler* and TESS are a promising method for detecting stellar activity cycles, since the flare rate for the Sun is observed to vary by roughly an order of magnitude between solar maximum and minimum (e.g. Veronig et al. 2002; Aschwanden & Freeland 2012). Long term monitoring of starspot modulations and rotation periods may also provide "butterfly diagram" estimates that can constrain activity cycles (e.g. Nielsen et al. 2019; Morris et al. 2019), or differential rotation (Reinhold et al. 2013; Davenport et al. 2015).

Here we explore the starspot and flare activity for GJ 1243 using a combination of light curves from *Kepler* and TESS that span a 10-year baseline. We introduce the newly released TESS short-cadence data in §2. In §3 we define our sample of flares from TESS, and compare the flare rate with the benchmark from *Kepler*. As in *Kepler*, two distinct starspots regions are found in the TESS light curves, and we explore their evolution over the past decade in §4. Finally we conclude with a look ahead at the promising future for stellar activity studies combining *Kepler* and TESS data in §5, and provide a brief summary of our results in §6.

2. TESS SHORT CADENCE DATA

TESS is a space-based, exoplanet-searching telescope that was launched in 2018. Over the course of the primary two-year mission, TESS will survey ∼85% of the entire night sky with at least 27 days of continuous observation in search of transiting exoplanets around the brightest nearby stars Ricker et al. (2014). To date, TESS has detected more than a thousand exoplanet candidates[1], while simultaneously studying the astrophysics of more than 200,000 stars with short-cadence (2-minute) data. The data from TESS Sectors 14 and 15 from mid-2019 (and again partially in mid-2020 with Sector 26) provide a unique opportunity to revisit the original *Kepler* field. By combining the data from both missions we can characterize stellar activity for GJ 1243 on a decade timescale[2].

We use the short cadence data from sectors 14 and 15, totalling 50.47 days of 2-minute observations. We are using the PDCSAP_FLUX light curves provided by the TESS mission directly, and require the Quality flag be set to 0 to ensure the highest fidelity data possible. Light curves for both Sector 14 and 15 are shown in Figure 1, with our detected flares (described below) highlighted.

3. COMPARING FLARE ACTIVITY

To gather a sample of flares from the TESS data, we examined the short cadence (2-minute) light curve for Sectors 14 and 15 using FBEYE Davenport et al. (2014). This flare finding suite was originally designed to manually build a pristine flare sample for GJ 1243 with *Kepler*. Flare candidates are first automatically located by detecting residuals from an iterative smoothing routine. We then performed a by-eye validation of the 50.47 day light curve, finding a total of 133 flare events.

Rather than flare energies, FBEYE provides the *equivalent duration* for each event, defined as the integral of the flare in zero-registered normalized flux, which has units of seconds (see Hunt-Walker et al. 2012). The energy for each flare is then determined by multiplying the equivalent duration by the luminosity. Following Davenport et al. (2016), we determined

---

[1] As of 2019 October, https://tess.mit.edu/publications/
[2] *Kepler* Quarter 0 was observed in May 2009

3
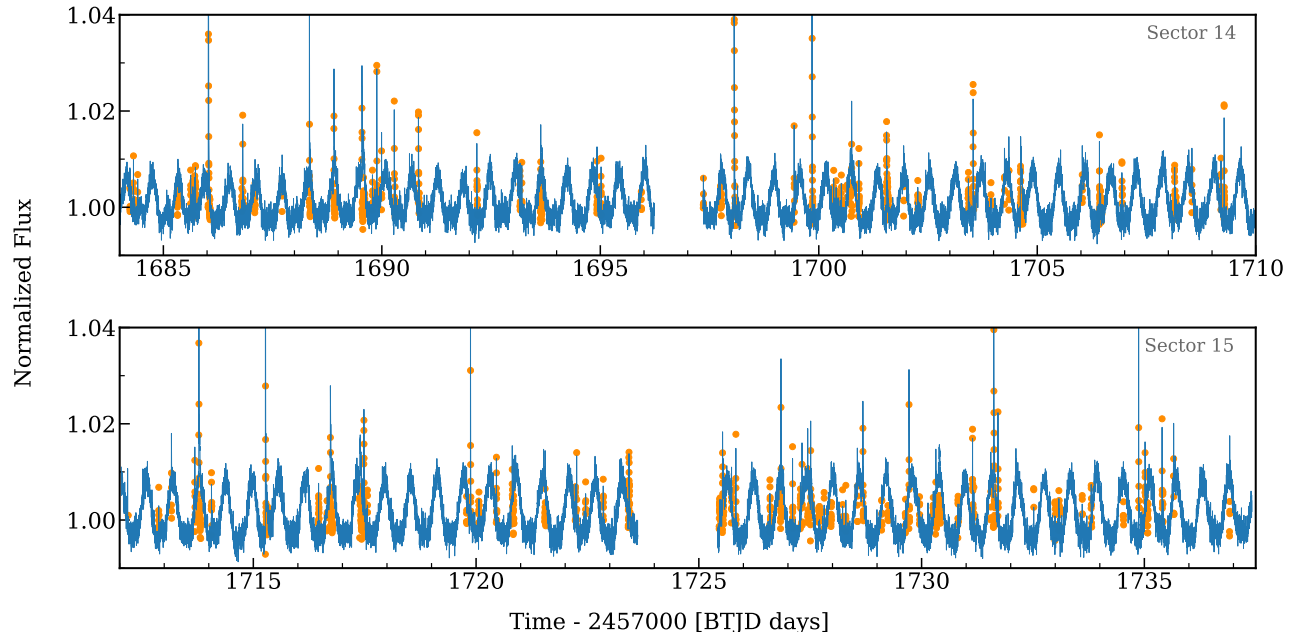
Figure 1. TESS Sector 14 and 15 light curves for the rapidly rotating, flaring M dwarf, GJ 1243. Using `FBEYE` we identified 133 flare events (orange points) over the 50 days of 2-minute cadence observations. For visual clarity we have not shown the full range of the largest detected flares, which reach ∼20% amplitudes.

the luminosity for GJ 1243 in both the *Kepler* and TESS bandpasses. As shown in Figure 2, each filter curve was convolved with the M4 NUV–NIR spectral template from Davenport et al. (2012), which was normalized to the flux-calibrated optical spectrum for GJ 1243 from Reid et al. (1995). We find L_{Kep} = 30.04 erg s^{-1}, and L_{TESS} = 30.35 erg s^{-1}. The *Kepler* luminosity used here is lower than the estimate from Hawley et al. (2014) due to the different flux-calibrated spectrum source. However, this does not impact our results in comparing the flare activity between *Kepler* and TESS. Rather, we note the importance of computing the luminosity for both bandpasses *consistently* when comparing flare rates between them.

Since the *Kepler* and TESS filter curves shown in Figure 2 cover different wavelength regions, we also briefly explored how comparable the flare energies determined using these two filters would be. We convolved a 10,000 K blackbody curve with each filter, since this is a typ-

ical flare temperature assumed when estimating flare energies. Though the *Kepler* filter is centered closer to the peak wavelength of this blackbody curve, the TESS filter's substantially wider wavelength coverage results in a 2.4% *larger* flux response. Given typical uncertainties in the distance estimation and flux calibration for nearby stars, this indicates TESS and *Kepler* have remarkably similar flare energy yields, and are well suited for comparison.
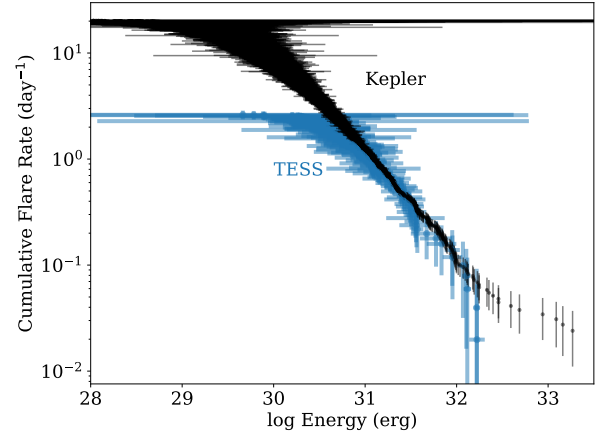
Flare frequency distribution (FFD) diagrams have been used to compare the occurrence rate of flares on stars as a function of flare energy (e.g. Lacy et al. 1976; Shibayama et al. 2013). This reverse sorted, cumulative flare distribution, characteristically shows many small energy events and very few high energy flares. Given their stochastic occurrence, FFDs help us understand the rate of flares over many orders of magnitude in event energy. Scoggins et al. (2019) used both FFDs and the integrated flare energy metric, L_{fl}/L_{Kep} introduced by Lurie
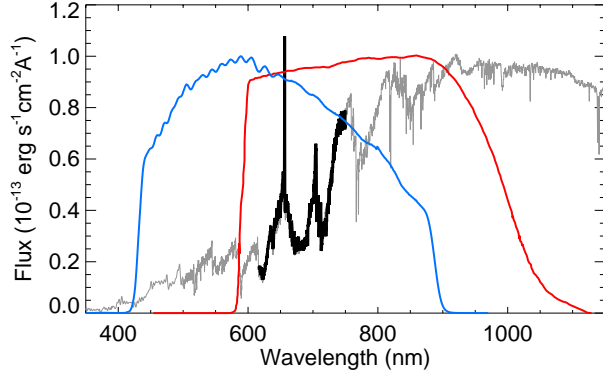
Figure 2. Flux calibrated spectrum for GJ 1243 (thick black line) from Reid et al. (1995), with scaled NUV–NIR M4 template (thin grey line) from Davenport et al. (2012), which is used to calculate the quiescent luminosity for GJ 1243 in the *Kepler* (blue line) and TESS (red line) bandpasses.

et al. (2015), to find flare activity variations within *Kepler* data. L_{fl}/L_{Kep} is a more robust measurement, as it averages over uncertainties in individual event energies, but assumes fixed observing conditions throughout the sample. As our flare data for GJ 1234 comes from two telescope surveys with substantially different apertures and observing baselines, FFDs are the best parameter space for comparing our flare activity levels (see §3 of Davenport et al. 2019).

Figure 3 shows the FFDs from the TESS and *Kepler* observations. The differences in turn over rates between the two data sets is correlated with the amount of data collected. The FFD for the TESS data includes 50.47 days worth of 2-minute observations, while the *Kepler* data spans 11 months short cadence, 1-minute monitoring. The apparently change in slope and rapidly increasing uncertainties at lower event energies are due to low signal-to-noise flares that have growing incompleteness in their recovery (Davenport 2016). For large energy flares we become limited by the observing duration, and are dominated by Poisson counting errors.

Figure 3. The cumulative flare frequency distribution (FFD) for the 6107 flares observed on GJ 1243 with *Kepler* (black line) from Davenport et al. (2014), and the 133 flares from TESS from this work (blue line). The flares are sorted from largest to smallest energy events per day. We can fit a power law to each data set (see section 3 for details). The turnover at low energies is due to lower detection efficiency of small flares.

Error bars shown for the FFDs in Figure 3 were produced following the approach of Davenport et al. (2016) and Howard et al. (2018). The uncertainty in the cumulative flare rates (y-axis) were computed using the Poisson upper-limit approximations from Gehrels (1986). Uncertainty in the flare energies were computed using a signal-to-noise ratio estimation for the equivalent duration, following the standard approach for equivalent widths in spectroscopy (Vollmann & Eversberg 2006). These energy errors have the correct behavior (i.e. errors decrease for higher energy events), but seem to over-estimate the uncertainty for the lowest energy (low S/N) flares. The combination of these occurrence rate and event energy uncertainties gives a characteristic "bow-tie" appearance to the FFD.

The FFD is typically modeled using a power law distribution, which has been shown to extend with a fixed slope over 10 orders of magnitude in flare energy for Solar-type stars for
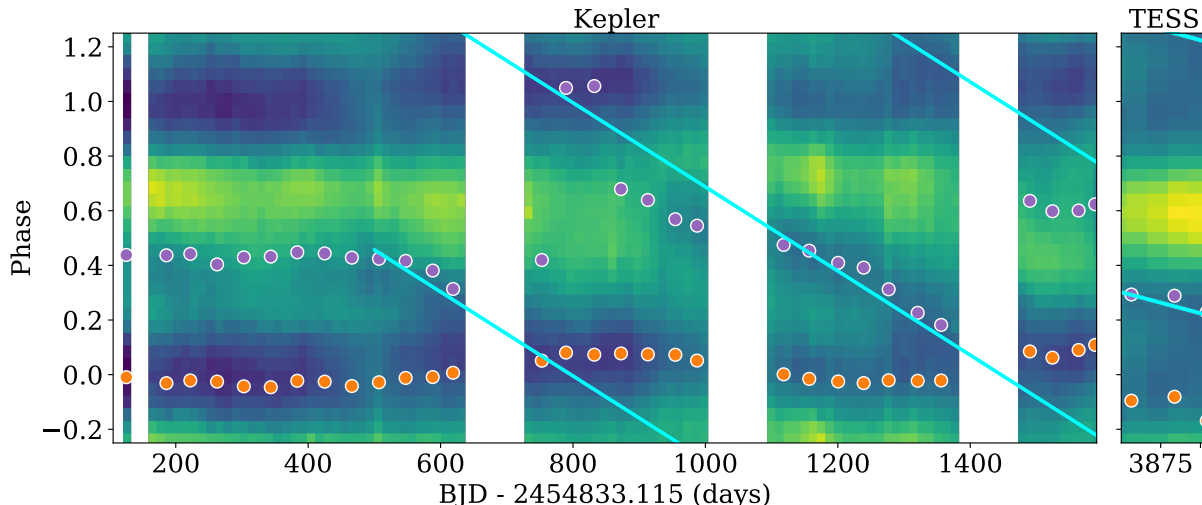
Figure 4. Mapping of relative flux (pixel shade, from dark to light) as a function of rotation phase and time for both the *Kepler* and TESS data of flux vs time and phase, following Davenport et al. (2015). The dark band centered at Phase=1 is the primary starspot group, which remains essentially unchanged over the entire 10 year dataset. Gaussian fits to the phase curves are used to trace the locations of the primary and secondary starspot in 40-day bins (orange and purple points). The differential rotation of the secondary starspot from Davenport et al. (2015) is fit from Time = 400 to 1400 days (blue line). Projecting forward to the TESS observations, the secondary spot appears in phase with this simple prediction, which is likely a coincidence.

"nanoflares" to "superflares" (Shibayama et al. 2013; Maehara et al. 2015). As noted in Scoggins et al. (2019), stars with significant differences in the power law *offset* (i.e the intercept in log-log space) would indicate changes in flare activity levels. A star whose flare activity level changed over a few year timescale may be undergoing activity cycles. We fit both the *Kepler* and TESS data with a linear model in log-log space. Within the resulting error uncertainties we find the FFDs for both the TESS and *Kepler* data are the same, revealing no sign of a stellar activity cycle over this decade. Our resulting power law fit for the TESS data was $\log_{10}(\nu) = -0.95 \pm 0.02 \times \log_{10} E + 29.4 \pm 0.7$, and for the *Kepler* FFD data was $\log_{10}(\nu) = -0.942 \pm 0.001 \times \log_{10} E + 29.27 \pm 0.04$. The larger uncertainties of the TESS data are to be expected, given the lower signal-to-noise of the light curves and the shorter duration of observation. However, it is encouraging that TESS

can effectively characterize the ongoing flare activity level of *Kepler* stars.

4. COMPARING STARSPOTS

Four years of nearly continuous monitoring for GJ 1243 from *Kepler* revealed the presence of two distinct starspot features, which appear as slowly evolving quasi-sinusoidal modulations in the light curve (e.g. Figure 1). Davenport et al. (2015) produced a detailed tracing of the phase (or equivalently, longitude) of both starspot features over the entire *Kepler* dataset. They noted the primary spot was approximately stable in both phase and amplitude, while the secondary feature evolved on a timescale of hundreds of days. Forward modeling of the *Kepler* light curve suggested the primary spot was located at a high latitude, while the secondary spot was at a lower latitude. Interestingly, during the final two years of the *Kepler* data, the secondary spot appeared to evolve almost monotonically in phase, which Davenport et al.

(2015) interpreted as the signature of differential rotation of a long-lived spot feature.

In Figure 4 we reproduce the phase versus time evolution map of flux from Davenport et al. (2015) for the 4-year *Kepler* long cadence (30-minute) data[3], as well as the new TESS Sectors 14 and 15 short cadence data. All data have been put onto the *Kepler* Barycentric Julian Date time. The combined *Kepler*–TESS 10-year light curve allows us to improve the rotation period estimation for GJ 1243. Using a Lomb-Scargle Periodogram, we measured the rotation period to be $P_{rot} = 0.5925974$ days, 1.2×10^{-6} days longer than the estimate from Davenport et al. (2015). Each Quarter of the *Kepler* long-cadence data has been normalized using the automated functions included in the `Lightkurve` package. Pixel color and shade encode the flux of the star as a function of time and rotational phase. The primary starspot is seen as a dark band (i.e. lower normalized flux in Figure 1) centered at Phase=0. Note we have increased the relative flux response of the TESS data here by a factor of 2 to approximately match the starspot amplitude seen in *Kepler*. This difference in spot amplitude is expected due to the redder wavelength center of the TESS filter (e.g. Figure 2), which leads to a lower spot-to-star contrast ratio (i.e. spots are higher amplitude at bluer wavelengths).

To analytically trace the positions of the starspots over the 10-year baseline, we have split the combined *Kepler*–TESS light curve into 40 day bins of time, and fit the phase-folded data within each bin with two Gaussian curves. The center phase of the primary and secondary spots are shown as circles in Figure 4. Modeling with Gaussian curves can cause blending and result in lower velocity amplitudes (this is often the case when decomposing multiple radial velocity

peaks in spectroscopy). The same effect can be seen here, with the two peaks blending together, causing the primary starspot position to "wiggle" in phase due to blending with the secondary spot.

Davenport et al. (2015) estimated the surface shear due to differential rotation by measuring a monotonic change in phase of the secondary starspot relative to the primary. Specifically, they focused on the clear evolution in the secondary spot seen in Figure 4 from Time ∼950 to ∼1400 days. We note if this evolution is propagated *backwards* in time, the spot feature around Time∼450 days appears to be in sync as well. However, as Davenport et al. (2015) found, the differential rotation evolution of this particular starspot does not correctly align with the secondary spot feature observed at Phase≈0.5 in the first ∼300 days of the *Kepler* data.

We updated the phase evolution estimate from Davenport et al. (2015) to include this earlier starspot, shown as a continuous blue line in Figure 4. As Davenport et al. (2015) illustrate, the negative slope of this line indicates a spot moving *faster* than the rotation period used to phase-fold the data. The actual slope of the linear fit is the inverse of the rotation lap time: $1/t_{lap} = -1.5393 \times 10^{-3}$, which can be converted to a rotation shear of $\Delta\Omega = 2\pi/t_{lap} = -0.00967$ rad day^{-1}, somewhat stronger than measured previously by Davenport et al. (2015).

We then propagated this updated differential rotation rate from *Kepler* to the new TESS observations, and find the secondary spot is at a phase consistent with the predicted phase. In Figure 5 we also find the the secondary spot appears to move slightly in phase between TESS Sector 14 and Sector 15 with the same shear rate seen in *Kepler*, while the primary feature remains at a fixed longitude. As seen in *Kepler*, the secondary spot in TESS also has approximately the same amplitude in the light curve,

---

[3] Here we used the final Data Release 25 version of the long cadence *Kepler* data
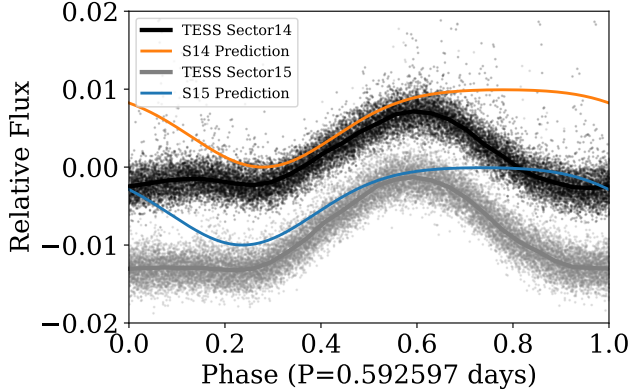
Figure 5. Phase-folded 2-minute cadence light curve TESS Sector 14 (black points) and Sector 15 (grey points) data for GJ 1243. The primary starspot from Davenport et al. (2015) at Phase=0 appears unchanged. The secondary starspot light curve, here modeled as Gaussian curves (orange and blue lines) in TESS Sectors 14 and 15 appears to track the phase location and evolution propagated from the *Kepler* data noted by Davenport et al. (2015).

indicating these starspots (or starspot groups) have roughly equal surface filling factors (areas).

The consistent location and evolution in phase of the secondary starspot seen in TESS as compared with *Kepler* has two possible interpretations: 1) this feature is the same starspot observed in the latter years of the *Kepler* mission, which has not changed significantly in latitude (i.e. change the differential rotation rate) or size relative to the primary spot. 2) The secondary spot seen in TESS is a newer feature than the one observed with *Kepler* and is coincidentally aligned with the predicted phase, but is likely at the same latitude since it exhibits the same differential rotation rate. Since we lack monitoring of GJ 1243 throughout the 6-year gap between the *Kepler* and TESS missions, it is impossible to show that a secondary starspot has remained consistent in its phase evolution throughout that time. As the secondary spot seen in the first 300 days of *Kepler* also does not appear to be in sync with this phase evolution,

we prefer the latter interpretation, that the secondary starspot seen in TESS is coincidentally in phase with the feature found in *Kepler*.

5. DISCUSSION

Using a combination of data from the *Kepler* and TESS missions we have analyzed space-based precision photometry spanning a 10-year baseline for the benchmark active M dwarf, GJ 1243. Our study of flaring and starspot behavior in these light curves sheds new light on the active lives of low-mass stars, and opens the door to searching for slow changes in flare rates due to activity cycles, or surface magnetic field topology via starspot modulations.

From the new sample of 133 flares from the 2-minute light curves in TESS sectors 14 and 15, we found the flare rate for GJ 1243 has not appreciably changed over the decade timescale. The raw number of flares detected per day is lower in TESS compared to *Kepler*, but this is simply due to the lower signal-to-noise in TESS, while the star's actual activity level was unchanged. As Davenport et al. (2019) notes, the Flare Frequency Distribution (FFD) is the most robust parameter space to compare flare activity levels between different stars or between observations of a given star with different noise levels or observing duration. The flare census for GJ 1243 shows no significant variation in either the gross flare rate, or the FFD slope, indicating the same physical process is at work. We also find that flare energies computed using the *Kepler* and TESS filters are comparable, making FFDs comparisons between these missions a prime tool in searching for flare rate variations.

The light curve for GJ 1243 shows a two-starspot morphology in both the *Kepler* and TESS data, with a rotation period and primary starspot feature that has remained unchanged over 10 years. This is similar to the stable starspot configuration seen for V374 Peg over a 16-year period from ground-based observations (Vida et al. 2016), but with much more de-

tailed tracing of the spot amplitudes and phase evolution. The long term stability of primary starspot in the new TESS data lends support to the interpretation that this feature represents a large polar spot "cap", possibly due to strongly dipolar magnetic field that is slightly misaligned with the rotation axis.

The secondary starspot for GJ 1243 has once again been observed to have weak differential rotation. While this secondary spot in TESS is perhaps coincidentally in phase with the evolution seen in *Kepler*, the 10-year spot map (Figure 4) indicates the surface is dominated by two very large, and very slowly evolving features. The presence of two such large and stable active regions poses interesting questions about the surface topology of the magnetic field for GJ 1243. We believe this benchmark star is a prime candidate for continued photometric monitoring, as well as follow-up spectro-polarimetric observations to constrain the surface magnetic field structure as was done for V374 Peg (Morin et al. 2008) and other late-type M dwarfs like GJ 1245B (Morin et al. 2010).

Hawley et al. (2014) found with *Kepler* that GJ 1243 showed now correlation between rotation phase and the flare rate or flare energy. This was interpreted as flares occurring in active regions across the entire star, rather than concentrated near the starspots. Using the TESS flare data we again find no indication of rotational phase correlation with flare occurrence or energy. By contrast, Roettenbacher & Vida (2018) have recently found that small flares *do* seem to occur coincidentally with major starspot groups for predominantly higher mass flare stars (G through M) in *Kepler*. They interpret this difference as a fundamental change in the surface magnetic topology, in agreement with dynamo models for convective stars (Yadav et al. 2015) that predict active regions (i.e. flares) are spread across the star's surface.

The constant flare rate and starspot properties for GJ 1243 broadly indicate that the star either lacks a solar-like activity cycle, or the timescale for such a cycle is much longer than 10 years. The latter interpretation is in conflict with the traditional view that long activity cycles correlate with slow rotation (Böhm-Vitense 2007). However, a lack of an activity cycle is not surprising given the possible young age for GJ 1243 (Silverberg et al. 2016), and that the star is rapidly rotating and well within the "saturated" dynamo activity regime where cycle behavior is not expected (e.g. see Testa et al. 2015). Long term monitoring for all active stars like GJ 1243 is now possible with missions like TESS. As Scoggins et al. (2019) notes this continuing flare rate census on decades timescales will be a valuable metric for detecting activity cycles for many stars.

6. SUMMARY

We have presented new flare rates and starspot tracing for the active M dwarf GJ 1243 from the TESS mission. Comparing with similar data from the *Kepler* mission allows an analysis of magnetic activity on a decade timescale. Both the flaring and starspot behavior appear unchanged, indicating no sign of an activity cycle. The primary starspot is found to be stable in phase, while the secondary starspot feature continues to show signs of weak, solar-like differential rotation.

We have found the flare rates and flare frequency distributions of M dwarfs between *Kepler* and TESS are easily compared, despite the significantly longer stare time and larger aperture of the former. The wider bandpass of the TESS filter results in a slightly larger ($\sim$2.4%) observed energy for a given flare as compared to *Kepler*– well within the nominal error budget of most flare energy estimates.

ACKNOWLEDGMENTS

REFERENCES

Aschwanden, M. J., & Freeland, S. L. 2012, ApJ, 754, 112

Astropy Collaboration, Robitaille, T. P., Tollerud, E. J., et al. 2013, A&A, 558, A33, doi: 10.1051/0004-6361/201322068

Böhm-Vitense, E. 2007, ApJ, 657, 486

Borucki, W. J., Koch, D., Basri, G., et al. 2010, Science, 327, 977, doi: 10.1126/science.1185402

Davenport, J. R. A. 2016, ApJ, 829, 23

Davenport, J. R. A., Becker, A. C., Kowalski, A. F., et al. 2012, ApJ, 748, 58, doi: 10.1088/0004-637X/748/1/58

Davenport, J. R. A., Covey, K. R., Clarke, R. W., et al. 2019, ApJ, 871, 241

Davenport, J. R. A., Hebb, L., & Hawley, S. L. 2015, ApJ, 806, 212, doi: 10.1088/0004-637X/806/2/212

Davenport, J. R. A., Kipping, D. M., Sasselov, D., Matthews, J. M., & Cameron, C. 2016, ApJL, 829, L31

Davenport, J. R. A., Hawley, S. L., Hebb, L., et al. 2014, ApJ, 797, 122, doi: 10.1088/0004-637X/797/2/122

Gehrels, N. 1986, ApJ, 303, 336

Giles, H. A. C., Collier Cameron, A., & Haywood, R. D. 2017, MNRAS, 472, 1618

Hawley, S. L., Davenport, J. R. A., Kowalski, A. F., et al. 2014, ApJ, 797, 121, doi: 10.1088/0004-637X/797/2/121

Howard, W. S., Tilley, M. A., Corbett, H., et al. 2018, ApJL, 860, L30

Hunt-Walker, N. M., Hilton, E. J., Kowalski, A. F., Hawley, S. L., & Matthews, J. M. 2012, PASP, 124, 545

Hunter, J. D. 2007, Computing In Science & Engineering, 9, 90, doi: 10.1109/MCSE.2007.55

Jones, E., Oliphant, T., Peterson, P., et al. 2001–, SciPy: Open source scientific tools for Python. http://www.scipy.org/

Lacy, C. H., Moffett, T. J., & Evans, D. S. 1976, ApJS, 30, 85

Lightkurve Collaboration, Cardoso, J. V. d. M., Hedges, C., et al. 2018, Lightkurve: Kepler and TESS time series analysis in Python, Astrophysics Source Code Library

Lurie, J. C., Davenport, J. R. A., Hawley, S. L., et al. 2015, ApJ, 800, 95

Maehara, H., Shibayama, T., Notsu, Y., et al. 2015, Earth, Planets, and Space, 67, 59

McKinney, W. 2010, in Proceedings of the 9th Python in Science Conference, ed. S. van der Walt & J. Millman, 51 – 56

Morin, J., Donati, J.-F., Petit, P., et al. 2010, MNRAS, 407, 2269

Morin, J., Donati, J.-F., Forveille, T., et al. 2008, MNRAS, 384, 77

Morris, B. M., Davenport, J. R. A., Giles, H. A. C., et al. 2019, MNRAS, 484, 3244

Nielsen, M. B., Gizon, L., Cameron, R. H., & Miesch, M. 2019, A&A, 622, A85

Oliphant, T. E. 2007, Computing in Science Engineering, 9, 10, doi: 10.1109/MCSE.2007.58

Pérez, F., & Granger, B. E. 2007, Computing in Science and Engineering, 9, 21, doi: 10.1109/MCSE.2007.53

Reid, I. N., Hawley, S. L., & Gizis, J. E. 1995, AJ, 110, 1838, doi: 10.1086/117655

Reinhold, T., Reiners, A., & Basri, G. 2013, A&A, 560, A4

Ricker, G. R., Winn, J. N., Vanderspek, R., et al. 2014, in Society of Photo-Optical Instrumentation Engineers (SPIE) Conference Series, Vol. 9143, Proc. SPIE, 914320, doi: 10.1117/12.2063489

Roettenbacher, R. M., & Vida, K. 2018, ApJ, 868, 3

Savanov, I. S., & Dmitrienko, E. S. 2011, Astronomy Reports, 55, 890

Scoggins, M. T., Davenport, J. R. A., & Covey, K. R. 2019, Research Notes of the American Astronomical Society, 3, 137

Shibayama, T., Maehara, H., Notsu, S., et al. 2013, ApJS, 209, 5

Silverberg, S. M., Kowalski, A. F., Davenport, J. R. A., et al. 2016, ApJ, 829, 129

Testa, P., Saar, S. H., & Drake, J. J. 2015, Philosophical Transactions of the Royal Society of London Series A, 373, 20140259

Veronig, A., Temmer, M., Hanslmeier, A., Otruba, W., & Messerotti, M. 2002, A&A, 382, 1070

Vida, K., Kriskovics, L., Oláh, K., et al. 2016, A&A, 590, A11

Vollmann, K., & Eversberg, T. 2006, Astronomische Nachrichten, 327, 862

Yadav, R. K., Gastine, T., Christensen, U. R., & Reiners, A. 2015, A&A, 573, A68